



22.2 % All-Aluminum Screen-Printed Silicon Solar Cells

Sebastian Junge^{1,*} , Byungsul Min¹ , Till Brendemühl¹ , Kosuke Tsuji² ,
Marwan Dhamrin^{2,3} , Henning Schulte-Huxel¹ , Verena Mertens¹ ,
and Rolf Brendel^{1,4} 

¹Institute for Solar Energy Research Hamelin (ISFH), Germany

²Toyo Aluminium K.K., Japan

³Graduate School of Engineering, Japan

⁴Dep. Solar Energy, Inst. Solid-State Physics, Leibniz University of Hannover, Germany

*Correspondence: Sebastian Junge, junge@isfh.de

Abstract. In this work, we present our current development status for all-aluminum screen-printed poly-Si on oxide p-type back junction solar cells. This cell type already features an aluminum front grid which forms locally p⁺-type layers to collect holes. For the rear side metallization, we use special aluminum-silicon (Al-Si) alloy pastes to locally contact the n⁺-type poly-Si after opening the dielectric layer by laser ablation. We compare two different glass frits (A and B) and two different concentrations of silicon in the pastes (low and high). Totally, three pastes are used for rear side metallization: (1) Al-Si paste with low Si and glass frit system A, (2) Al-Si paste with low Si and glass frit system B and (3) Al-Si paste with high Si and glass frit system A. The front and rear side of our solar cells were printed and fired separately. The glass frit system B in paste 2, results in reduced shunt resistance of below 5 kΩ·cm², negatively influencing the open circuit voltage. The high silicon content in paste 3 prevents local shunting in the cells, consequently reducing the series resistance and leading to a fill factor gain of more than 3 %_{abs} compared to the other pastes. Our best Ag-free solar cell shows a power conversion efficiency of 22.2 % with an open circuit voltage of 718 mV and was printed using the high-Si amount paste. In a simulation-based synergistic efficiency gain analysis, we identify the rear side recombination at the contacts and the front grid shading as the two dominant factors.

Keywords: Aluminum, Silver-Free, Poly-Silicon on Oxide

1. Introduction

The manufacturing of contemporary high-efficient silicon solar cell types such as tunnel oxide passivated contact (TOPCon) or silicon heterojunction (SHJ) solar cells is heavily reliant on silver (Ag) for the purpose of electrical contacts on both sides. Given the anticipated expansion of the photovoltaic (PV) industry, a further increase in the consumption of silver is expected in the coming years. This trend poses significant ecological and economic risks [1] and underscores the urgent need for the development of alternatives to silver pastes. Since aluminum (Al) is an abundant and cheap metal, and Al pastes already found their way into the well-established screen-printing technology [2], one logical way would be to simply substitute Ag pastes with Al pastes. However, Al pastes come with two major concerns: high shading loss due to wide finger width and easy alloying to silicon.

The shading loss can be partly overcome by our poly-Si on oxide (POLO) back junction (BJ) solar cells [3]. Its lateral hole conductivity is given by the p-type wafer itself, allowing for 2 mm pitched and over 60 μm wide Al fingers on the front side – an advantage not given by a front junction cell design such as PERC or TOPCon cells. POLO BJ cells have achieved 24.2 % power conversion efficiency, with screen-printed Ag-fingers contacting the rear side poly-Si [4].

For this study, the rear-side Ag paste was replaced with Al pastes from the TTC series of TOYO Aluminium K.K [5]. Beside different glass frit systems we also investigate the impact of different Si amount in Al paste on contacting n⁺-type poly-Si to avoid the violent reaction between the n⁺-type poly-Si and Al pastes [6]. We investigate two different glass frit systems (A and B) and two different concentrations of Si (high and low). In total, three pastes were used for the rear side metallization. They are listed in Table 1, as well as their relevant compositions.

Table 1. Al-pastes and their respective glass frit systems and Si concentrations.

| Al-paste | Glass frit system | Silicon concentration |
|----------|-------------------|-----------------------|
| Paste 1 | A | Low |
| Paste 2 | B | Low |
| Paste 3 | A | High |

In contrast to our previous work [2], we apply a fully covered rear side metallization instead of a grid design in order to overcome the low conductivity of the aluminum alloy powders. Furthermore, we investigate the performance of our cells in a simulation based synergistic efficiency gain analysis (SEGA) [7] to identify dominant loss mechanisms.

2. Experimental

The POLO BJ cells fully metalized with aluminum, as seen in Figure 1, are produced from 156.75 mm \times 156.75 mm (M2) gallium-doped Cz silicon wafers. First, they are etched from saw damage and cleaned, before an oxide layer is thermally grown on both sides. Then, *in-situ* phosphorus-doped poly-Si layers are deposited using a low-pressure chemical vapor furnace. The thickness of the n⁺-type poly-Si is 450 nm. Afterwards, 20 minutes oxidation at 900 °C leads to the formation of POLO junctions and creates a protective layer of additional oxide on top of the n⁺-type poly-Si. This oxide was removed on one side – the later front side – *via* laser ablation. A texturing and cleaning step removed the front side n⁺-type poly-Si as well as the rear side protective oxide, and formed pyramids on the front side. Both sides were passivated with a stack of $\text{AlO}_x/\text{SiN}_y$ by a plasma enhanced chemical vapor deposition furnace.

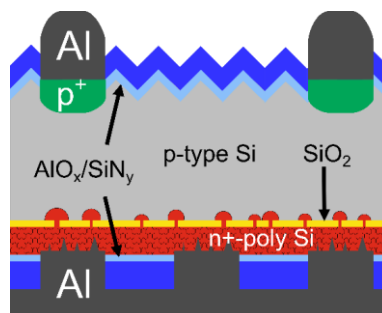


Figure 1. Schematic of a POLO BJ solar cell with rear full area screen printed Al and front Al fingers.

The metallization of our cells was conducted in separate steps for the front and the rear side. First, all cells received laser contact opening (LCO) by a picosecond laser at the front side, followed by screen-printing of a busbar-less finger grid of conventional aluminum paste, TB series, and firing at a peak temperature of 790 °C. By that, the local p⁺-type regions were

formed at the front side. Afterwards, LCO was applied on the cells' rear side. This step is necessary, because the Al pastes do not fire through the passivation stack of AlO_x and SiN_y . The different rear side pastes were applied via screen-printing in a full rear side covering structure. Afterwards firing was conducted at 710 °C, which was found out to be the highest possible temperature without causing severe damage to the n^+ -type poly-Si by the Al pastes. The finished cells were measured in our in-house LOANA tool from pvtools by applying a contacting scheme that neglects the resistance of the metal grid [8].

3. Results

3.1 Impact of rear side Al paste on IV data

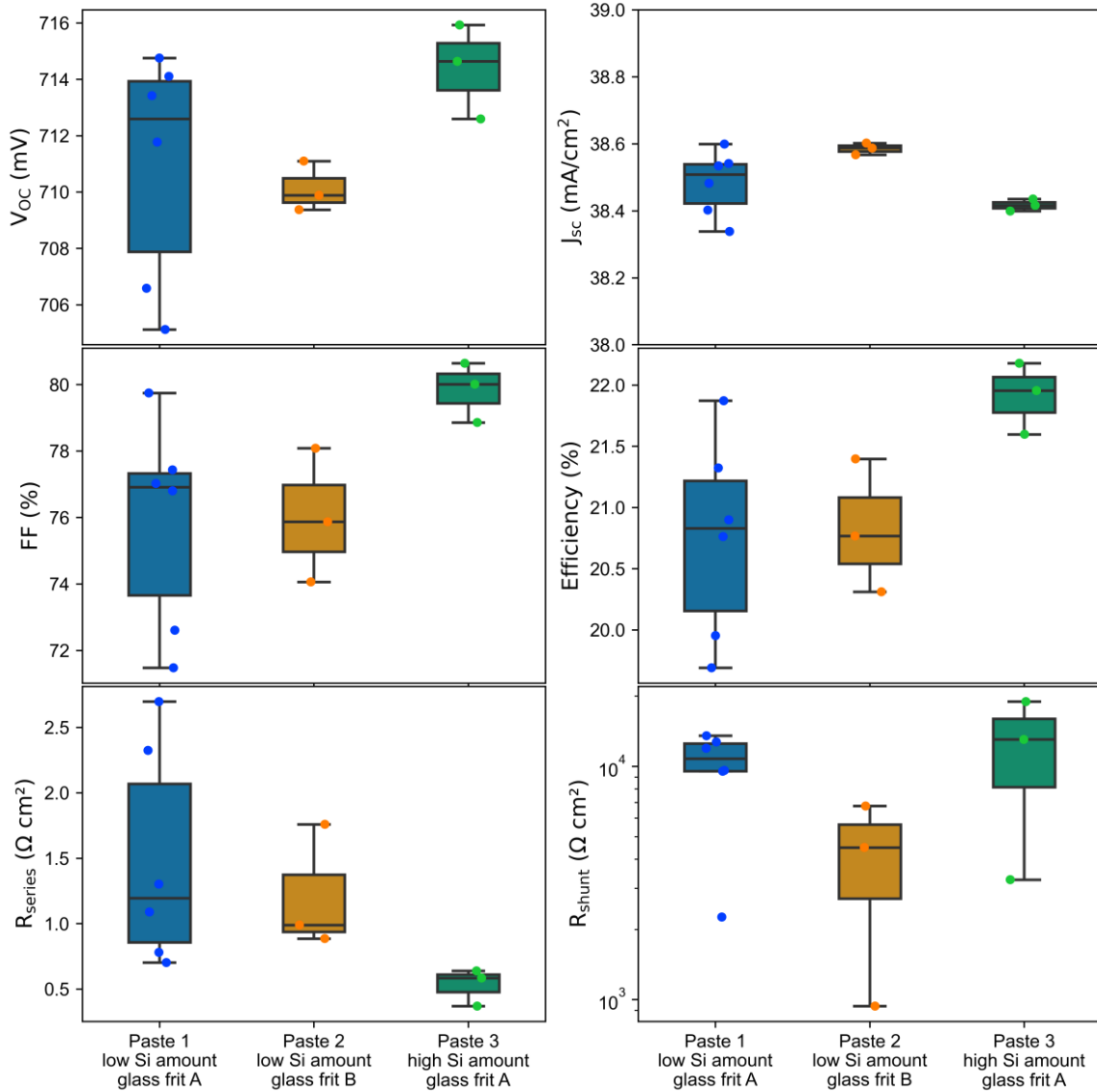


Figure 2. IV-parameters of Ag-free POLO BJ solar cells with fully metallized rear side as a function of rear side Al paste.

Figure 2 shows the IV parameter of our Ag-free POLO BJ cells with full rear metallization as a function of the used Al paste at the rear side. The median V_{OC} of cells printed with paste 1 is 713 mV, while cells with paste 2 have a median V_{OC} of 710 mV, and cells with paste 3 have a median V_{OC} of 715 mV. The results indicate a slightly higher deterioration or damage to the n^+ -type poly-Si layer, suggesting the failure of glass frit system B. This glass system promotes a

reaction between Al and the poly-Si layer, leading to local Al spiking, which in turn reduces the shunt resistance. This is reflected in the shunt resistances of $10.8 \text{ k}\Omega\cdot\text{cm}^2$, $4.5 \text{ k}\Omega\cdot\text{cm}^2$, and $13 \text{ k}\Omega\cdot\text{cm}^2$ for pastes 1, 2, and 3, respectively. These relatively low values are indicative of local shunts across the back junction at the rear contacts, which we attribute to Al spiking.

Furthermore, our findings demonstrate that an increased silicon content in Al pastes results in an enhanced fill factor, which can be attributed to a lower series resistance of $0.58 \text{ }\Omega\cdot\text{cm}^2$ for paste 3 as compared to $1.2 \text{ }\Omega\cdot\text{cm}^2$ for paste 1. We reason that the higher amount of Si in the Al paste regulates the alloying process of Al and Si and therefore reduces reactions between the paste and the n^+ -type poly-Si. The utilization of a high Si amount in our Ag-free POLO BJ cells metalized with two different Al pastes has yielded a median efficiency enhancement of approximately $1.1 \text{ \%}_{\text{abs}}$ when compared to the reference paste, which possesses a lower Si amount.

To further investigate the presence of local shunts at the rear contacts we removed the Al wet-chemically and investigated the regions of LCOs with a scanning electron microscope (SEM). Figure 3 shows damaged areas of n^+ -type poly-Si for the example of a cell, which was screen-printed with the paste 3. Local shunts were formed where the Al spiked through Si, even though the paste had a high amount of Si. Preventing such spikes is a crucial step towards high efficiency all-aluminum solar cells and might require alternative methods for metal-semiconductor contacting, which supports contact formation at lower firing temperature.

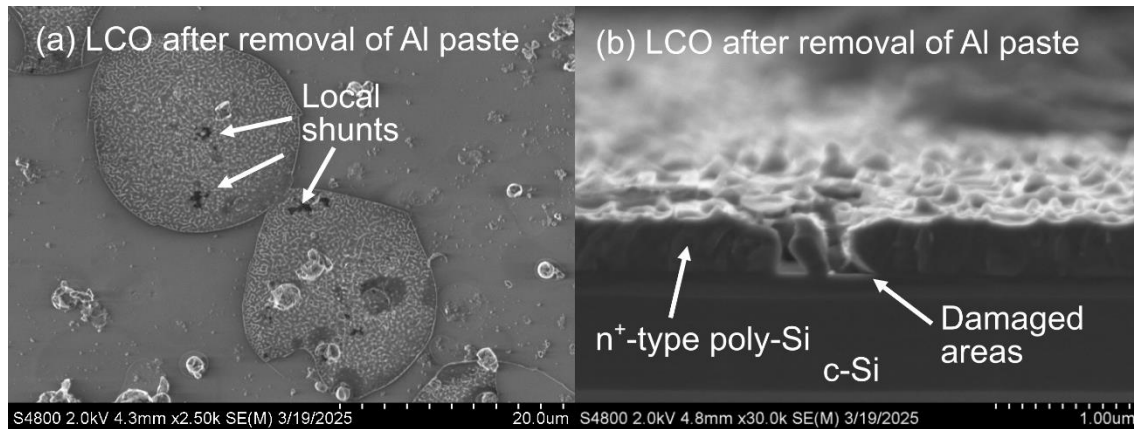


Figure 3. SEM images of rear side contacts after removal of Al. Exemplary LCOs from (a) top view and (b) side view.

Our results showcase the feasibility of highly efficient screen-printed silver-free POLO BJ solar cells with manufacturing processes standardized for industry. An increased silicon content facilitates contact formation at the emitter resulting in relative high efficiencies of 22 %. Our best cell achieves a V_{OC} of 718.3 mV, an FF of 79.08 % and an efficiency of 22.2 %, independently confirmed by ISFH CalTeC (Figure 3) and was contacted with paste 3.

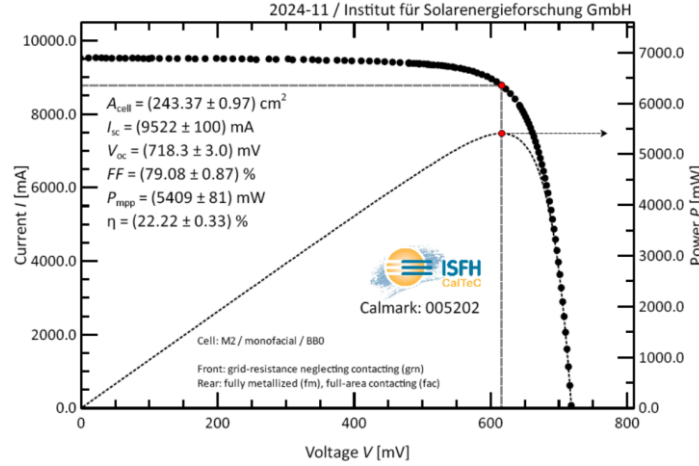


Figure 4. IV-results of our best cell, independently measured by ISFH CalTeC.

3.2 Synergistic efficiency gain analysis

To quantify potential improvements of our cell efficiencies, we performed a SEGA of the best cell, which we modelled in the simulation software Quokka3 [9] which uses conductive boundary model [10]. Table 1 lists the input parameter used for the simulation. Values for J_0 , τ_n and τ_p were fitted to the lifetime curve of an unmetallized precursor. We extract recombination current densities $J_{0, \text{pass}}$ of passivated surfaces by reproducing the measured injection-dependent lifetime curves from test structures without metallization. We then vary the recombination current density at the rear metal contact $J_{0, \text{met, rear}}$ to reproduce the measured IV parameters. As the recombination current density at the front metal contact $J_{0, \text{met, rear}}$, we apply a constant value which was determined in our previous work [4]. To account for potentially shunting the cell's junction beneath the rear metal contacts, we also implement $J_{02, \text{rear}}$ in our simulations. The injection-dependent lifetime curves are measured with the Sinton lifetime tester WCT-120. The contact resistance ρ_c was measured with a TLM-SCAN from pvtools.

Table 2. Input parameters for the simulation of our best Ag-free POLO BJ cell in Quokka3.

| Parameter | Value |
|-----------------------------|-------------------------------|
| ρ_{Bulk} | 1.17 $\Omega \text{ cm}$ |
| $\tau_{n0, \text{SRH}}$ | 1.207 ms |
| $\tau_{p0, \text{SRH}}$ | 63.845 ms |
| $\rho_{c, \text{front}}$ | 0.984 m $\Omega \text{ cm}^2$ |
| $J_{0, \text{pass, front}}$ | 3.57 fA/mc 2 |
| $J_{0, \text{met, front}}$ | 870 fA/cm 2 |
| $R_{\text{sheet, emitter}}$ | 25.9 Ω/\square |
| $\rho_{c, \text{rear}}$ | 5.23 m $\Omega \text{ cm}^2$ |
| $J_{0, \text{pass, rear}}$ | 2.58 fA/mc 2 |
| $J_{0, \text{met, rear}}$ | 30 fA/cm 2 |
| $J_{02, \text{met, rear}}$ | 300 $\mu\text{A/cm}^2$ |

As demonstrated in Figure 5, the SEGA of our best cell identifies the most dominant loss channels as the contacted recombination J_{02} and the optical losses due to the front grid's shading. To reduce the optical losses, the application of nodeless screens may lead to thinner Al front fingers. The contact formation process at the rear side is very sensitive to LCO power and firing temperature (data not shown) and therefore is a suitable target for further contact enhancing methods.

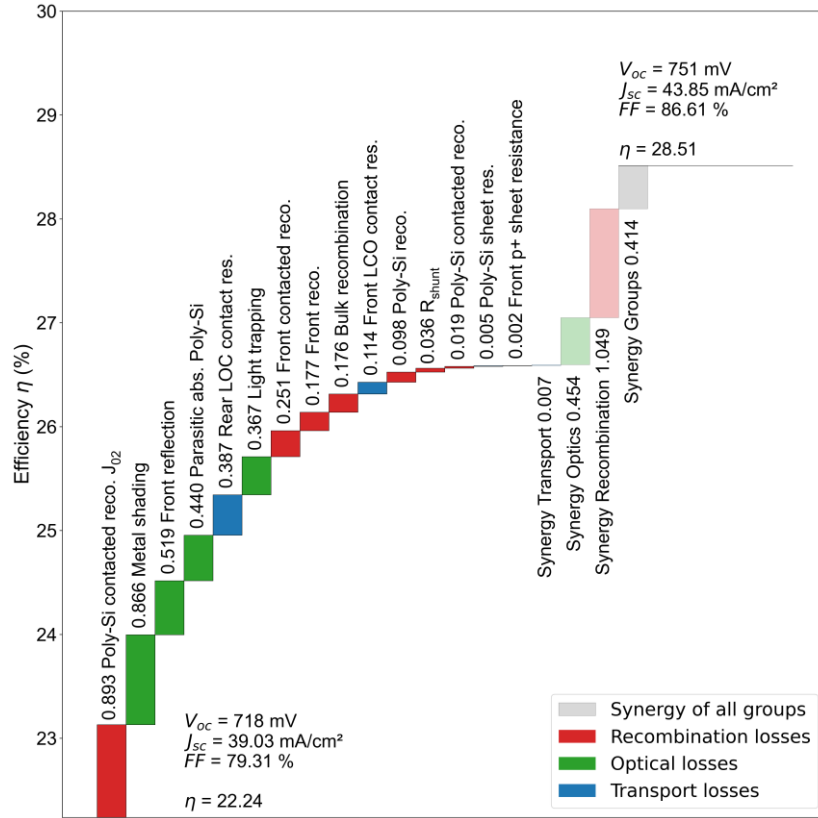


Figure 5. SEGA of the best cell.

4. Conclusion

This work demonstrates our recent progress made in the production of silver-free solar cells. The study demonstrates the efficacy of screen-printed Al pastes in establishing contact with n⁺-type poly-Si at the rear side of POLO BJ cells. Furthermore, it investigates the influence of different glass frit systems and Si amount Al paste on the cells' performance. Our findings indicate enhanced contact formation in high Si amount conditions. Our best all-aluminum screen-printed cell shows an efficiency of 22.2 % and a V_{OC} of 718 mV.

Additionally, our findings indicate, that – beside optical losses – the formation of rear side contacts is a dominant source of loss. That includes the recombination J_{02} as well as contact resistance between the n⁺-type poly-Si and screen-printed paste. Consequently, future advancements in all-aluminum POLO BJ cells should prioritize the investigation of Al/n⁺-type poly-Si interface contact mechanisms.

Author contributions

S. Junge: Conceptualization, Methodology, Validation, Formal analysis, Investigation, Writing – original draft, visualization; B. Min: Conceptualization, Methodology, Validation, Formal analysis, Investigation, Writing – review & editing, project administration, funding acquisition; T. Brendemuehl: Methodology, Writing – review & editing; Kosuke Tsuji: Conceptualization, Methodology; Marwan Dhamrin: Conceptualization, Methodology, Writing – review & editing; H. Schulte-Huxel: Conceptualization, Writing – review & editing; Verena Mertens: Conceptualization, Writing – review & editing; R. Brendel: Writing – review & editing, supervision

Competing interests

The authors declare that they have no competing interests.

Funding

This work is funded by the Federal Ministry for Economic Affairs and Climate Action under grant no 03EE1150A.

Acknowledgement

The authors thank to M. Pollmann, B. Gehring, L. Spasowka, S. Spaetlich, T. Friedrich and T. Neubert for processing samples, B. Gehring for SEM measurements (all ISFH). This work was financially supported by the German Federal Ministry for Economic Affairs and Climate Action (BMWK) under contact number 03EE1150A (APOLON).

References

- [1] B. Hallam *et al.*, "The silver learning curve for photovoltaics and projected silver demand for net-zero emissions by 2050," *Progress in Photovoltaics*, vol. 31, no. 6, pp. 598–606, Jun. 2023, doi: [10.1002/pip.3661](https://doi.org/10.1002/pip.3661).
- [2] B. Min *et al.*, "All-Aluminum Screen-Printed POLO Back Junction Solar Cells," 40th European Photovoltaic Solar Energy Conference and Exhibition, pp. 020044-001-020044-004, 2023, doi: [10.4229/EUPVSEC2023/1CV.3.2](https://doi.org/10.4229/EUPVSEC2023/1CV.3.2).
- [3] B. Min *et al.*, "A 22.3% Efficient p-Type Back Junction Solar Cell with an Al-Printed Front-Side Grid and a Passivating n + -Type Polysilicon on Oxide Contact at the Rear Side," *Solar RRL*, vol. 4, no. 12, p. 2000435, Dec. 2020, doi: [10.1002/solr.202000435](https://doi.org/10.1002/solr.202000435).
- [4] B. Min *et al.*, "24.2% efficient POLO back junction solar cell with an AlOx /SiNy dielectric stack from an industrial-scale direct plasma-enhanced chemical vapor deposition system," *Progress in Photovoltaics*, vol. 33, no. 1, pp. 236–244, Jan. 2025, doi: [10.1002/pip.3828](https://doi.org/10.1002/pip.3828).
- [5] S. Suzuki *et al.*, "SCREENPRINTED ALUMINIUM CONTACTS on N+-DOPED SILICON," in 37th photovoltaic conference proceedings, online-conference, 2020.
- [6] Y. Ding *et al.*, "22.56% total area efficiency of n-TOPCon solar cell with screen-printed Al paste," *Solar Energy*, vol. 280, p. 112862, Sep. 2024, doi: [10.1016/j.solener.2024.112862](https://doi.org/10.1016/j.solener.2024.112862).
- [7] R. Brendel, T. Dullweber, R. Peibst, C. Kranz, A. Merkle, and D. Walter, "Breakdown of the efficiency gap to 29% based on experimental input data and modeling," *Progress in Photovoltaics*, vol. 24, no. 12, pp. 1475–1486, Dec. 2016, doi: [10.1002/pip.2696](https://doi.org/10.1002/pip.2696).
- [8] K. Bothe, *et al.*, "Contacting of busbarless solar cells for accurate IV measurements," in *Proc. 37th eur. Photovolt. Sol. Energy conf. Exhib.*, 2020, pp. 277–281.
- [9] A. Fell, *et al.*, "The concept of skins for silicon solar cell modeling," *Solar Energy Materials and Solar Cells*, vol. 173, pp. 128–133, Dec. 2017, doi: [10.1016/j.solmat.2017.05.012](https://doi.org/10.1016/j.solmat.2017.05.012).
- [10] R. Brendel, "Modeling solar cells with the dopant-diffused layers treated as conductive boundaries," *Progress in Photovoltaics*, vol. 20, no. 1, pp. 31–43, Jan. 2012, doi: [10.1002/pip.95](https://doi.org/10.1002/pip.95)